AIAA 79-7004R

Air-Inlet Engine Matching Problems Encountered in a Jet Trainer Re-engining Program

Sridhar M. Ramachandra,* K. Sudhakar,† P.V.K. Perumal,‡ and P. Jayasimha§
Hindustan Aeronautics Limited, Bangalore, India

An advanced jet trainer re-engining program was undertaken at Hindustan Aeronautics Limited by using a derated engine. The present paper describes the theoretical and experimental investigations carried out both on ground and in flight into the flow-induced catastrophic blade vibration/flutter consequent upon the usage of an initial air induction channel configuration. The revised air channel design philosophy for suppressing flow separation and reducing static and dynamic distortions, resulting in prolonged blade life and improved engine performance, is also outlined.

Introduction

ENGINE-airframe compatibility is critical for both civil and military high performance aircraft. There is a close correlation between the flowfield characteristics in the inlet capture area and the resultant flow characteristics at the compressor face. Flowfield examinations have shown local flow angles of attack and yaw far in excess of the aircraft geometric attitude angles. Since the inlet flow is influenced strongly by the external airframe geometry, it is necessary to study their effects on the local flow directions and the nonuniformities of the incoming flow to obtain an understanding of the airframe-inlet interactions. In this connection Zonars[1] reports the results of systematic experimental investigations on a family of fuselage configurations over a Mach number range from 0.8 to 2.5, angle-of-attack range from -3 to $+24$ deg and side-slip angles from -4 to $+4$ deg, including the effects of two wing sweep angles.

Inlet flow distortions reduce the stall margin and, hence, the surge margin of the highly loaded compressor regions, thereby reducing the acceleration margin. Besides, flow distortions increase the maximum gas turbine inlet temperature and also increase the blade vibratory stress levels. The magnitude and pattern of these flow distortions also depends substantially on the flight Mach number, engine air mass flow and the angles of attack and side slip. Attainment of uniform velocity distribution at the compressor and design of engines of increased distortion tolerance are two possible solutions to overcome these problems. It may be mentioned here that a high recovery inlet may not always have a low distortion. It fact, as Manganiello mentions during discussions of Alford's paper,[2] a high recovery inlet is generally more sensitive to off-design operation and, hence, may give higher distortion levels over a range of operation than a lower recovery inlet. A bell-mouth air inlet imparts a uniform velocity distribution at the compressor face with minimal pressure loss, whereas actual air ducts have curves, bends, and aerodynamic losses that diminish the pressure recovery and cause flow distortion at the compressor face. Early air induction system designs were governed only by the acceptable radial and circumferential variation bounds for the steady-state dynamic pressure/total pressure at the compressor face prescribed by the manufacturer. The inadequacy of this simple criterion has been demonstrated by the recent experiment on intake development at Hindustan Aeronautics Limited for a single-engine, high-speed jet trainer aircraft in a re-engining program by replacing it with a derated higher thrust engine. Total pressure surveys in the originally designed air channel showed the presence of severe large-scale flow unsteadiness that affected the engine performance adversely.

The importance of considering the unsteady nature of inlet flows has also been realized elsewhere through its profound effect of reducing the stability margins of compressors, leading to compressor stall. In subsonic flight, inlet diffusor flow separation could cause flow unsteadiness. Inlet pulsations in supersonic flight may arise from shock-wave boundary-layer interactions, causing flow separation and random spatio-temporal inlet flow turbulence.

Inlet turbulence has a wide range of amplitude-frequency content, in general. When the disturbances are of low frequency, the engine performance follows a very similar pattern to that of the steady state so that the outlet pressure will be in phase and the overall compression ratio remains the same. When the inlet pressure fluctuations are of high frequency, the exit pressure lags behind the inlet variations both in phase and amplitude so that the overall compression ratio may differ significantly from the steady-state value until the flow conditions so develop as to nullify the stall margin completely. Subsonic flight inlet diffusor flow separation and supersonic flight shock-wave boundary-layer induced interactions may produce unsteady flow distortions which affect the engine behavior, causing dynamic instabilities. Zonars[1] reports NASA Lewis and AEDC experiments on inlet flow fluctuations showing reduction of the compressor surge margin, the margin decreasing rapidly with increasing turbulence level.

Although the present study relates to velocity/pressure distortions only, it may not be out of place to mention Abdel Wahab's recent[3] experimental work on temperature transients and their effects on a turbofan engine such as would arise during gun firing. He found that the Pratt & Whitney TF 30-P-3 turbofan engine compressor could tolerate temperature transients without instability below certain levels of temperature change depending on the magnitude of the temperature change, the circumferential extent of temperature distortion, rate of temperature rise, and the low pressure rotor speed. The effect of temperature

Presented as Paper 79-7004 at the 4th International Symposium on Air Breathing Engines, Walt Disney World, Fla., April 1-6, 1979; submitted June 19, 1979; revision received June 24, 1981.

*Deputy Chief Designer (Technology and Analysis); present address: Professor, Department of Aeronautical Engineering, Alfateh University, Tripoli, Libya.
†Project Engineer.
‡Design Engineer.
§Project Engineer.

transients on turbojet engines has also been reported earlier by Gabriel et al.[4]

An 11.1-kN-thrust Bristol Siddeley Viper engine had been used to power the aircraft C to meet its advanced jet trainer role requirements. The 18.7-kN-thrust Bristol Orpheus engine used to power the jet fighter B was derated to 15.6-kN thrust to replace the Viper engine of C to adapt it to the COIN role designated here as aircraft C2 with an initial air intake configuration C2-I. The present paper describes the theoretical and experimental investigations carried out both on ground and in flight consequent upon the catastrophic flow-induced inlet guide vane vibration/flutter experienced during this re-engining program. The revised air channel design philosophy to suppress the flow separation and reduce the spatio-temporal flow nonuniformity, resulting in considerable engine performance improvement and compressor blade fatigue life augmentation, is presented here.

Air Channel Design

Figure 1 shows the cross-section area distribution of the initial air channel C2-I compared with that of aircraft B using the same engine. Subsequent to the inlet guide vane failure, the air channel redesign was started with nylon tuft observations of the flow quality in the intake diffusor C2-I together with dynamic/total pressure surveys at the compressor face. These showed the presence of extensive diffusor flow separation causing the flow unsteadiness and the severely fluctuating large negative pressures that led to the unsatisfactory engine performance and the blade flutter failure. Thus, in addition to the steady-state radial and circumferential inlet flow distortions, dynamic distortions were also present. A survey of the steady-state and instantaneous distortion indices[5-8] represented by Rolls-Royce, Pratt & Whitney, and General Electric formulations indicated that although their formulations were different, they were all statistically similar. In this paper the Rolls-Royce definition of distortion indices will be used.

Rolls-Royce expresses the overall and the circumferential steady-state flow distortion indices DI_0 and DI_c, respectively, as

$$DI_0 = (V-\bar{V})/\bar{V} \qquad DI_c = (V-\bar{V}_r)/\bar{V}_r \tag{1}$$

where $\bar{V}$ is the compressor face mean velocity based on mean flow and annulus area; V is the local velocity at any point of the compressor face; and $\bar{V}_r$ is the average velocity for a particular ring of radius r.

For the Bristol Orpheus 701 engine, DI_0 and DI_c are subject to the limits

$$-0.15 \le DI_0 \le 0.15 \qquad -0.05 \le DI_c \le 0.05 \tag{2}$$

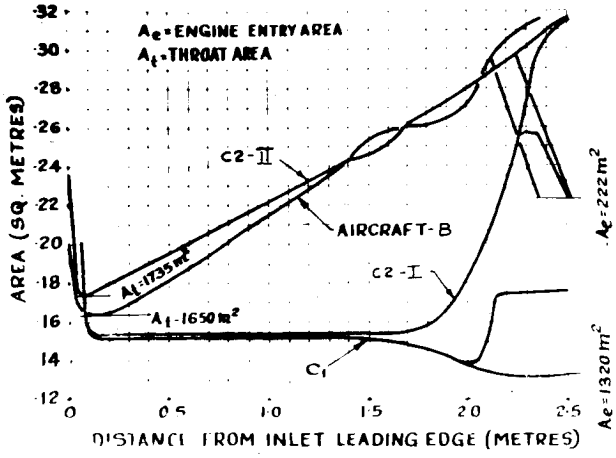

Fig. 1 Area distribution along the air channel.

as specified by the manufacturers. Rolls-Royce also defines a total pressure distortion index DC_{60} in terms of its variation over any 60-deg annular sector of the compressor face by

$$DC_{60} = [(P_{\min})_{60\,\deg} - P_{0E}]/\bar{q} \tag{3}$$

where P_{0E} is the mean total pressure, $(P_{\min})_{60\ \deg}$ is the minimum mean total pressure over any 60 deg sector of the annulus and $\bar{q} = \frac{1}{2}\rho\bar{V}^2$ is based on the mean velocity $\bar{V}$ at the compressor face.

The negative pressures (total pressure-static pressure) encountered were considered indicators of the magnitude and intensity of a flow separation in the original air channel C2-I. Total pressure surveys revealed the separated flow region to be near the 0- and 180-deg positions of the Inlet Guide Vane (IGV) plane looking into the compressor face with the separation intensity increasing with the engine rpm. The flow separation was related to the large channel divergence angle over the last 1-m length of the duct, resulting in both the flow quality deterioration and pre-entry losses increasing with the rpm at these angular positions. Hence the channel C2-I (entry area = 0.204 m^2) was replaced within the geometric constraints of the aircraft by the channel C2-II (entry area = 0.233 m^2) to reduce the pre-entry losses with $dA/dx > 0$ and nearly constant along the channel (Fig. 1). The possibility of flow separation in channel C2-II was checked by using the momentum integral equation,[9] Eq. (4), and Garner's equation,[9] Eq. (5), given by

$$(d\Theta/dx) + \Theta\{(a+x)^{-1} + [(H+2)/U](dU/dx)\} = \tau_0/\rho U^2 = 0.0065\,(U\Theta/\nu)^{-1/6} \tag{4}$$

$$(U\Theta/\nu)^{1/6}\Theta(dH/dx) = -[(\Theta U/\nu)^{1/6}(\Theta/U)(dU/dx) + 0.0135(H-1.4)]\exp 5(H-1.4) \tag{5}$$

which were solved simultaneously by the Runge-Kutta-Gill method for the momentum thickness Θ and the shape factor H (Fig. 2). In this method, since a precise value of H for three-dimensional flow separation is not defined and H has a wide spread varying from 1.8 to 3.0, only a rapid increase in H can be considered a possible criterion for the onset of separation.

An alternative method would be to relate the channel length and the channel cross-section areas for separation-free flow in a three-dimensional duct. Although the critical area ratio $\mathfrak{A}_{cr} = A_2/A_1$ for flow separation in a three-dimensional channel is not available, for a two-dimensional flow it is given by[10]

$$\mathfrak{A}_{cr} = l + 0.3001l + 0.0493l^2 - 0.0776l^3 + 0.0176l^4 \tag{6}$$

where

A_1 = diffusor inlet area
A_2 = diffusor exit area
l = l/b_1
l = diffusor length = 0.46 m C2-I
= 2.19 m C2-II
b_1 = channel width at the entry = 0.45 m C2-I
= 0.47 m C2-II

Assuming the two-dimensional critical area ratio will introduce a slight conservativeness in the design, the condition for separation-free channel flow may be written as

$$\mathfrak{A} \le \mathfrak{A}_{cr} \tag{7}$$

Using this condition for the air channel C2-I, the critical part of the duct was the last 1-m length for which $\mathfrak{A} = 1.62$ as compared to $\mathfrak{A}_{cr} = 1.3$, indicating the possibility of

Table 1 Comparative distortion indices of aircraft A, B, C1 and C2 from ground runs

Aircraft	rpm, %	Mean velocity $\bar{V}$, kmh	DI_c, circumferential % Max	DI_c, circumferential % Min	DI_r, radial % Max	DI_r, radial % Min	DI_0, overall % Max	DI_0, overall % Min
B	90	483	10.30	−14.90	11.00	−23.25	11.00	−24.00
A	...	...	26.30	−17.70	...	...	23.00	−24.70
C2-II	...	359	10.36	−16.94	21.23	−16.20	12.34	−22.35
C1	95	409	22.80	−37.00	14.90	−23.50	17.20	−32.40
B	...	544	11.50	−11.05	12.90	−18.00	12.40	−18.30
A	...	...	22.00	−24.10	...	...	27.00	−34.50
C2-II	98	375	12.00	−20.00	21.95	−18.70	11.11	−25.93
C2-II	...	384	12.75	−18.88	23.50	−17.70	15.60	−25.30
C1	100	431	27.40	−40.40	19.50	−26.30	19.80	−44.20
B	...	569	14.46	−16.79	17.14	−24.21	14.52	−26.50

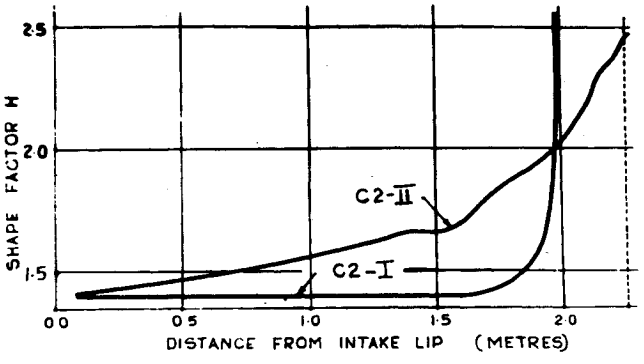

Fig. 2 Variation of shape factor along the duct chamber.

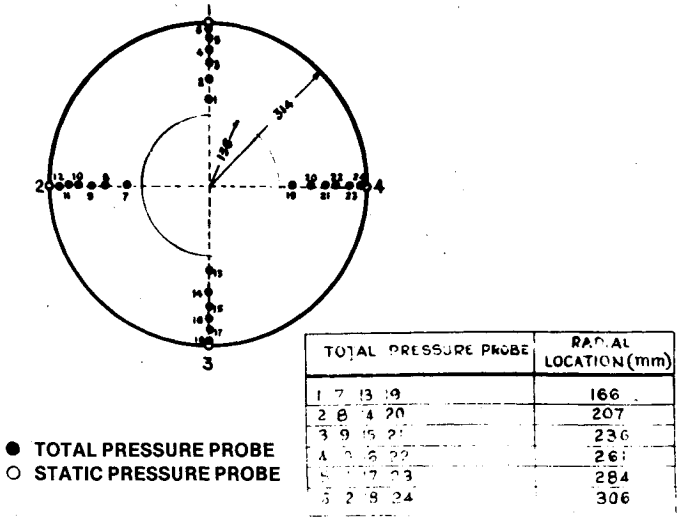

Fig. 3 Location of pressure probes.

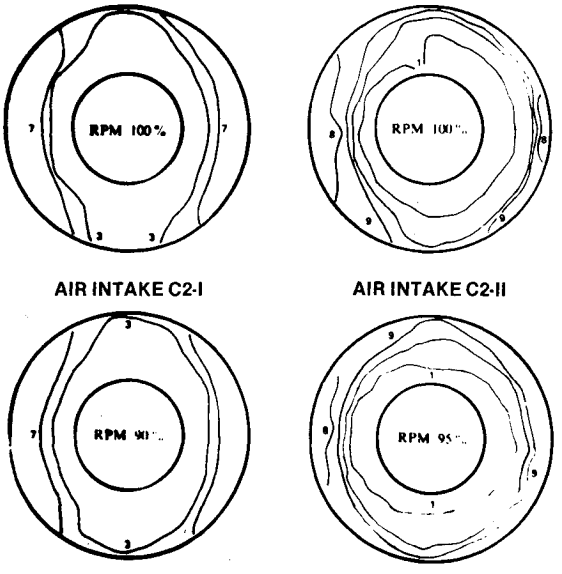

Fig. 4 Isovelocity contours, ground run.

separation. But, channel C2-II has a gradual diffusion over the entire length with $\mathcal{A} = 1.71$, whereas $\mathcal{A}_{cr} = 3.92$, indicating no possibility of flow separation.

Measurements and Analysis

Pressure measurements were made in channels I and II of the aircraft C2 both on the aircraft and on the jet engine test bed on which the derated engine performance was checked out before installation on the aircraft. The pressures were measured ahead of the compressor face with a 24 tube total pressure rake (four vanes with six probes in each) and four static pressure probes (Fig. 3) with a 10-Hz frequency response scanivalve and were used to compute the steady-state values. The steady-state flow quality is indicated by the circumferential and overall distortion indices DI_c and DI_0, Eq. (1). Table 1 shows a comparison of the measured steady-state distortion indices DI_c and DI_0 of the air channels I and II, with those of aircraft A and B (aircraft A is a fighter powered by a minor variant of the Bristol Orpheus 701 engine, the Orpheus 703) using the same engine. The steady-state velocity distortions are shown graphically as dimensionless isovelocity contours over the compressor face in Figs. 4 and 5.

Continuous in-flight pressure records, with a 50-Hz frequency response pressure transducer at one of the total pressure points, showed a dominant 32-Hz frequency in the flow fluctuation spectrum. Continuous total pressure records were also obtained at the 0-deg position with a 10-psi, 300-Hz frequency response pressure transducer, since it was one of the locations of severe fluctuation. The velocity fluctuation spectrum at the other points of the compressor face may be assumed to be nearly the same or similar to that at the 0-deg location, although possibly of a somewhat lower intensity. The real-time analyzer spectral records of these velocity fluctuations are shown in Fig. 5 with the ratio $P_{trms}/\bar{P}_t$ based on the rms values of the fluctuations up to 300 Hz listed in

Table 2. Measurements of the IGV natural frequency with the engine off and the dominant frequency at which they were excited for various rpm's are shown in Table 3.

Discussion of Results

The comparative steady-state isovelocity contours (Figs. 4 and 5) show considerably improved flow uniformity in channel C2-II compared to channel C2-I in which the low energy fluid of the separated zone was present near the outer edges of the annulus on the horizontal plane along with the high velocity regions close to the hub. Channel C2-II also shows nearly circular isovelocity contours and an increasing level of uniformity and reduced steady-state distortion index with forward speed in comparison with the stationary condition. Thus the low velocity regions are sparse. The isovelocity contours of channel C2-II for 95 and 100% rpm show an increasing degree of concentricity with reduction of the engine rpm, whereas no conclusions can be drawn on channel C2-I owing to the diffusor flow separation. Table 1 shows that the steady-state distortion indices for the channel C2-II are of the same level as on aircraft B and much better than on aircraft A. Benefits of flow quality improvement in channel C2-II have also manifested themselves through a reduced jet pipe temperature of the derated engine (Fig. 6). A possible explanation for this observation may be the fact that improvement of the inlet velocity profile through reduction of the distortion indices over the compressor face causes increased air mass flow rate and retards the rate of deterioration of the velocity profiles over the radius as the flow passes downstream through the various compressor stages. Besides improvement of the compressor work done factor, the increased mass flow rate leads to an increased thrust and a reduced TET (Turbine Entry Temperature) and JPT (Jet Pipe Temperature).

The steady-state velocity distortion indices for the channels C2-I and C2-II calculated from the compressor surface velocity measurements obtained during both ground runs and in flight at a flight speed of 450 kmph IAS (Indicated Air Speed) are given in Figs. 4 and 5. Magnitudes of the compressor face inlet velocities have been obtained from the pitot rake, assuming the plenum chamber static pressure of the intake diffusor is equal to the local static for both the channels. However, the accuracy of the isovelocity contours for C2-I could not be gaged owing to the presence of diffusor flow separation which vitiated correct total pressure measurement. Nevertheless, improvement of the isovelocity contours and the distortion indices for the channel C2-II is definite.

Improved flow steadiness in channel C2-II is evident also from the absence of violent pressure fluctuations and low instantaneous flow distortions (Fig. 7). Spectral analysis of the fluctuating components exhibits many interesting features (Fig. 8). In combination with a bell-mouth intake on the engine test bed, two dominant high frequency components can be identified, corresponding to the engine rotational speed and its second harmonic together with an unaccounted minor 380-Hz peak and several low frequency peaks, including a 50-Hz supply frequency component that was present at all engine

Table 2 Comparative dynamic pressure measurements on air channels with Orpheus 701 engine

	On engine test bed			On aircraft
$P_{trms}/\bar{P}_t$, rpm	Bell-mouth intake	B	C2-I	C2-II
4000	0.2780	0.3590	0.098	0.3735
7500	0.0239	0.1250	0.380	0.1229
8000	0.0210	0.1180	0.478	0.1171
8500	0.0158	0.1140	0.563	0.1200
8750	0.0129	0.1144	0.619	0.1239
9000	0.0119	0.1029	0.703	0.1048

Table 3 Comparative vibration levels of inlet guide vanes of Orpheus 701 engine

Location,		B		C2-I		C2-II	
deg	rpm	Hz	dB	Hz	dB	Hz	dB
210	8000	255	22	345	23	270	14
210	9000	243	25	345	25	258	14
150	8000	268	26	335	24	285	18.5
150	9000	270	28	335	29	283	19
30	8000	280	26	...	...	290	18.5
30	9000	280	30	...	...	288	23
330	8000	243	23.5	300	16	250	18
330	9000	243	26	300	21	248	18

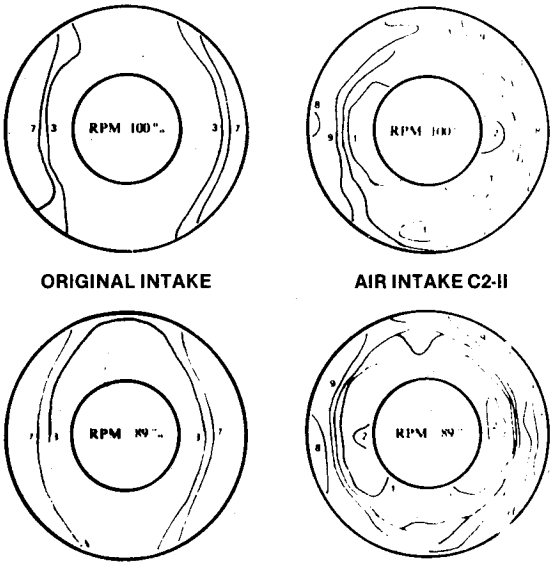

Fig. 5 Isovelocity contours V, 450 kmph.

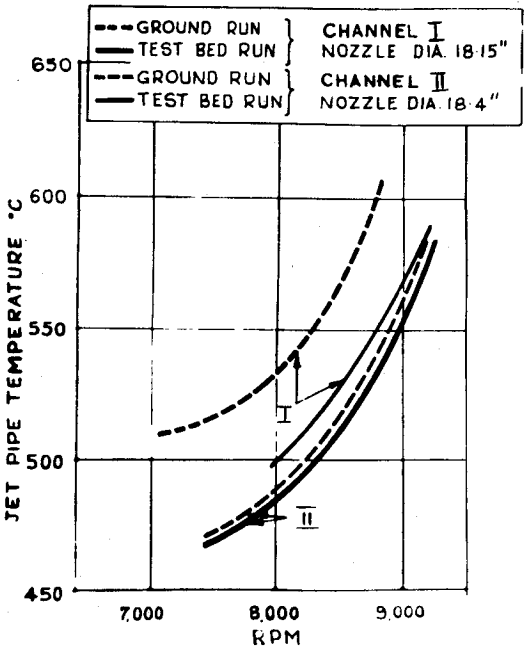

Fig. 6 Comparison of JPT's.

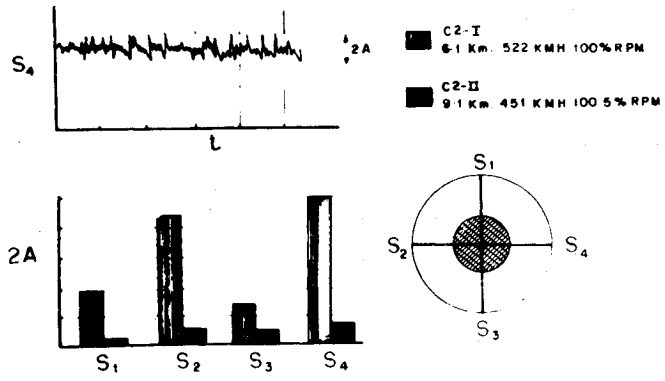

Fig. 7 Intensity of static pressure fluctuations.

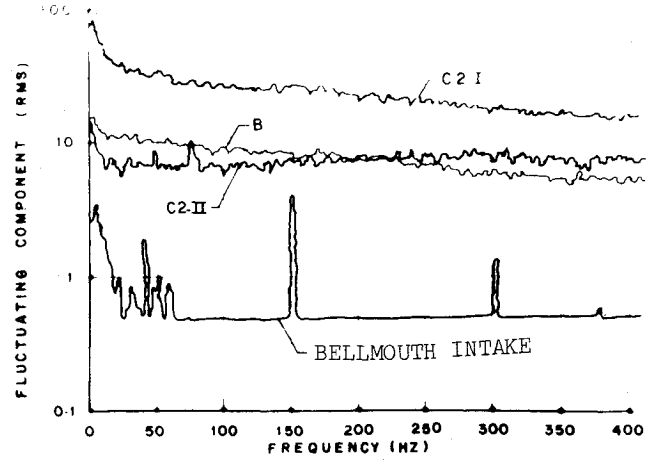

Fig. 8 Spectral composition, engine rpm 9000.

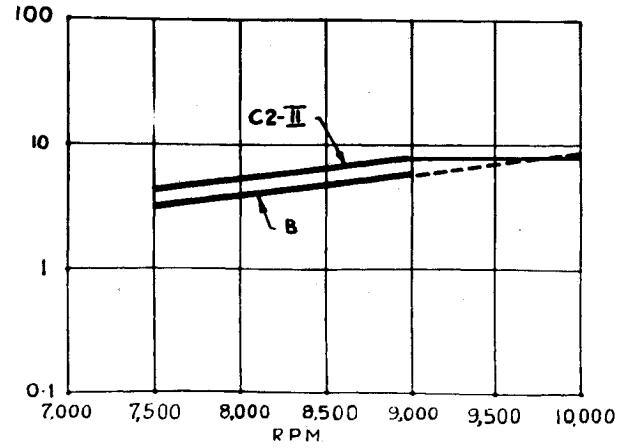

Fig. 9 Root mean square fluctuation level for aircrafts C2-II and B in the frequency range 0-300 Hz.

rpm's. In contrast, engine test bed measurements on the same engine but separately with the air channel C2-I and that of the aircraft B showed the presence of a broadband noise with no duct resonance or other conspicuous frequencies. The spectra of the fluctuations in these three channels show the same frequency composition over the observed frequency range with a distinct variation in the energy content, as seen from the different rms levels (Fig. 8). The engine blade passage frequency and the supply frequency components, although present here too, are, however, not conspicuous owing to the generally increased overall noise level.

Steady-state distortions have no ill effects on the inlet stator guide vanes but do affect the aerodynamic loading over the compressor rotor blades adversely. As each blade crosses a region of maximum total pressure into a low total pressure region, the aerodynamic loading on the blade undergoes a rapid change from a maximum to a minimum, the number of these fluctuations depending on the number of total pressure peaks and troughs present at any given radius of the compressor face. If in addition, the air channel flow is also subject to temporal unsteadiness, both the stator and the compressor rotor blades will be subject to unsteady aerodynamic loads whose spectrum consists of the instantaneous distortion spectrum of the flow. Consideration of the effects of dynamic or instantaneous distortions becomes, therefore, important.

The observed frequent loosening of the IGV's and the eventual failure of one of them on the aircraft may be ascribed to the separation-induced flow unsteadiness in channel I of aircraft C2. The IGV natural frequency is close to 300 Hz (Table 3). It is of interest to compare the energy fluctuation level E over a 300-Hz bandwidth for the various air channels. For this purpose, the rms fluctuation amplitude ratio R may be defined by

$$R = \text{rms fluctuation amplitude ratio} = \frac{(\text{rms fluctuation})_{\text{I}}}{(\text{rms fluctuation})_{\text{II}}} = R_{\text{I}}/R_{\text{II}} \tag{8}$$

for the two air channels. Over a frequency bandwidth from 0 to 300 Hz, $R = 3.85$, which is close to an rms energy ratio $E = R^2 = 14.8$, since $E \sim R^2$. Figure 9 shows the rms fluctuation level R increasing with the engine rpm.

The basic Orpheus 701 engine of the aircraft B, which operates at a maximum rpm of 10,000, was derated by restricting its maximum rpm to 9000 for use on the aircraft C2. The rms fluctuation level on the aircraft B air duct as measured on the engine test bed at 90% rpm is $R_{\text{B}} = 10.3\%$, which is close to $R_{\text{II}} = 10.5\%$ measured in channel II of aircraft C2 at 9000 rpm. Precise values of the corresponding rms fluctuation levels R_{I} for channel C2-I are not available except that measurements have shown $E_{\text{I}} > 50\text{-}100\%$ at 9000 rpm. A comparison of the fluctuation levels R_{B} of aircraft B and R_{II} shows that $R_{\text{B}} > R_{\text{II}}$ at 100% rpm although $R_{\text{B}} < R_{\text{II}}$ at lower rpm's. Furthermore, the amplitude and frequency of the IGV vibration as measured on the engire test bed with the engine running between 7500-9000 rpm are shown in Table 3 using the intake duct of aircraft B, the air channel C2-I with welded inlet guide vanes, and the channel C2-II with the rubber bonded blades of aircraft C2. Significantly reduced vibration levels with the channel C2-II and the rubber bonded vanes are evident compared to the channel C2-I and the aircraft B intake. In this respect, the modified air channel of C2, the channel C2-II, may be considered superior to that of B.

The maximum mass flow rate of aircraft B at 10,000 rpm is 38 kg/s while that of C2 at 9000 rpm is 34 kg/s after deration. Consequently, the maximum channel mean airspeed $\bar{V}_{\max}$ at the compressor face on aircraft B is 140 m/s compared to 124 m/s on aircraft C2. Therefore the mean normal bending stress level $\bar{\sigma}$ of the IGV's and that of the first- and second-stage compressor blades is much higher in aircraft B than on C2, being proportional to $\bar{V}^2_{\max}$, owing to the aerodynamic loads. Besides, because of a 10% reduction in the maximum rpm in the derated engine, the normal stresses due to the centrifugal forces are 19% lower in the derated engine blades compared to the basic Orpheus 701 engine. Consequently, the combined mean stress level $\bar{\sigma}$ due to the lower mean flow velocity $\bar{V}_{\max}$ and the reduced rpm is 21.5% smaller on aircraft C2 than on B.

Again, considering the air channel velocity fluctuations, we see that the absolute rms velocity fluctuation level in channel

II of aircraft C2 is also slightly higher than on aircraft B. Since $R=3.85$, as seen above, $R_{II}=0.2597\ R_I$ on aircraft C from Eq. (8). The stress level fluctuations on the blades of the IGV and the first and second stages of the compressor, however, are proportional to $E=R^2$ for a given mean stress level determined by $\bar{V}_{max}$. Since $E=14.8$, it is evident that $\sigma'_{II}=0.0676\ \sigma'_I$, where σ' is the stress fluctuation. Although measurement of channel airspeed fluctuations on aircraft B are not available, they may be expected to be similar to R_{II} on aircraft C2.

For life estimation of the derated Orpheus 701 engine compressor blades in combination with the air channel II, it is sufficient to consider only the effects of the inlet guide vanes and the blades of the first and second stages of the compressor. The other compressor stages need not be considered since steady-state and instantaneous distortions of the duct flow will normally have, at most, second-order effects on the other stages owing to blade row interference and the inertial effects of fluid in the rotor which attenuate the inlet distortions.[11] The energy fluctuation level E in channel I of aircraft C2 was high enough to produce a large stress level fluctuation σ' about an estimated mean stress level $\bar{\sigma}=1336$ kgf/cm^2 in the IGV, causing early failure of the IGV's after 8 h of engine run ($\sim 8.64^6$ cycles), whereas actual experience has shown that the IGV's on aircraft B have a very long life. In comparison, although the mean stress level $\bar{\sigma}$ of the aircraft B with the air channel II remain the same, since the stress level fluctuations are proportional to E and are small, the blade fatigue life is almost infinite. Furthermore, the considerably lower stress levels of the compressor stages, due to the reduced rpm and mass flow, will not affect their fatigue life adversely.

The operational characteristics of the Orpheus 701 engine show that during a steady-state operation, the compressor does not approach surge limits between sea level and 9100-m altitude. In regard to the transient operation, the adjustment of the slam timing for acceleration from 3250 to 6800 rpm has further reduced the possibility of compressor surge.

References

[1] Zonars, D., "Problems in Inlets and Nozzles," ICAS Paper 70-47 presented at the 7th Congress of the International Council of Aeronautical Sciences, Rome, Sept. 1970.

[2] Alford, J.S., "Inlet Duct-Engine Flow Compatibility," *Proceedings of the 5th International Aeronautics Conference*, Los Angeles, Calif., June 1955, pp. 504-516.

[3] Abdel Wahab, M., "Effects of Temperature Transients at Fan Inlet of Turbofan Engine," NASA TP 1031, Sept. 1977.

[4] Gabriel, D.S., Wallner, L.E., and Lubic, R.J., "Some Effects of Inlet Pressure and Temperature Transients on Turbojet Engines," *Aeronautical Engineering Review*, Vol. 16, Sept. 1957, pp. 54-59.

[5] Jacocks, J.L. and Kneile, K.R., "Statistical Prediction of Maximum Time Variant Inlet Distortion Levels," AEDC-TR-121, Jan. 1975; also, NTIS Rept. AD/A-004 104.

[6] Burcham, F. W. Jr. and Hughes, D.L., "Analysis of In-Flight Pressure Fluctuations Leading to Engine Compressor Surge in an F-111A Airplane for Mach Numbers to 2.17," AIAA Paper 70-624, June 1970.

[7] Costakis, W.G., "Experimental Investigation of a Simple Distortion Index Utilizing Steady State and Dynamic Distortion in a Mach 2.5 Mixed Compression Inlet and Turbofan Engine," NASA TMX-3169, 1977.

[8] Plourde, G.A. and Brimelow, B., "Pressure Fluctuations Cause Compressor Instability," Air Force Airframe/Propulsion Compatibility Symposium, June 1969.

[9] Schlichting, H., *Boundary Layer Theory*, McGraw Hill Book Company, New York, 1968.

[10] Chang, Paul K., *Separation of Flow*, Pergamon Press, New York, 1970.

[11] Tamada, Y., "Inlet Distortion and Blade Vibration in Turbomachinery," *Proceedings of the 2nd International Symposium on Air Breathing Engines*, Sheffield, England, March 1974.